

Precursors linked via the zipper-like structure or the filopodium during the secondary fusion of osteoclasts

Jiro Takito^{1,2,*} and Masanori Nakamura¹

¹Department of Oral Anatomy and Developmental Biology; School of Dentistry; Showa University; Tokyo, Japan; ²Research Center of Supercritical Fluid Technology; Graduate School of Engineering; Tohoku University; Sendai, Japan

Keywords: actin, cell-cell interaction, filopodia, fusion, osteoclast, podosome, superstructure

Abbreviations: DC-STAMP, dendritic cell-specific transmembrane protein; DIC, differential contrast; EGFP, enhanced green fluorescent protein; RANKL, receptor activator of NFκB ligand

We previously reported the transient appearance of an actin superstructure, called the zipper-like structure, during the primary fusion (fusion of mononuclear precursors) and the secondary fusion (fusion of multinucleated cells) of osteoclasts. Here, we focus on the actin-based superstructures that link two precursor cells during the secondary fusion event. In one type of secondary fusion, the osteoclasts transformed the podosome belts into the zipper-like structure at the site of cell contact and the apposed plasma membranes in the zipper-like structure attached to each other via a discontinuous interface. In another type of secondary fusion, the osteoclasts used a filopodium-like protrusion that linked the two cells. Both types of cell fusion required a lag period between the adhesion of the cells and the fusion of cell bodies. Thus, the secondary fusion of osteoclasts uses actin-based superstructures for cell-cell interactions before the definitive fusion of the plasma membranes.

Osteoclasts are multinucleated cells that resorb bone, and alterations in this activity have been associated with bone diseases, including osteoporosis. The cytokine RANKL (encoded by *Tnfsf11*) converts mononuclear cells of monocyte/macrophage lineages into fusion-competent mononuclear cells, and cell fusion of the competent cells results in a multinucleated osteoclast.^{1,2} The degree of multinucleation correlates with the bone-resorbing activity of osteoclasts. Although it is known that DC-STAMP, a putative seven-transmembrane protein, is essential for the fusion,^{3,4} little is known about how DC-STAMP participates in the fusion of osteoclasts.

By monitoring the rearrangement of the actin cytoskeleton during osteoclastogenesis, we previously found the transient expression of an actin-rich superstructure during cell fusion.⁵ We called it the zipper-like structure, because it morphologically resembled the adhesion zipper found in keratinocytes. To create a stable epithelial sheet, epithelia link to their neighboring cells by forming adherence junctions and tight junctions. In the initial stage of adherence junction formation, epithelia reorganize the assembly of actin filaments at the site of cell contact:^{6,7} this reorganization produces a prominent actin superstructure, called the adhesion zipper, in the filopodial processes of keratinocytes.⁸ During the maturation of cell contact, the adhesion zipper seals the gap between the two cells and disappears in the established

adherence junction. Because such actin-based superstructure is also observed in fibroblasts, the adhesion zipper might represent the conserved organization of actin during homotypic cell adhesion.

A podosome is a small spot-like actin-based superstructure mainly found in cells of monocyte/macrophage lineages and v-Src transformed cells.^{9,10} The podosome is composed of a dense actin core containing Arp2/3, cortactin and gelsolin surrounded by a loose actin cloud containing integrins, vinculin and paxillin. Proteomic analyses estimate the number of components of the integrin adhesome, a relative of the podosome, to be approximately 100 ~ 200.^{11,12} Such component diversity must guarantee the dynamics of the podosome. In osteoclasts, podosomes reorganize into a large ring-like superstructure called the podosome belt on a glass. Osteoclasts in bone form a sealing zone, which is roughly equivalent to the podosome belt. The sealing zone is a cell-matrix adhesion machinery that creates an isolated space between the cell and the matrix for bone resorption.¹⁰ Similar to the podosome, the podosome belt is composed of two functionally distinct domains: the podosome core and integrin-containing adhesion domain.¹³ The rearrangement of podosome-derived superstructures in osteoclasts depends on external cues, and the differentiation signal by RANKL spontaneously induces the transformation of podosomes into the podosome belt.¹⁴ The

*Correspondence to: Jiro Takito; Email: takito@dent.showa-u.ac.jp

Submitted: 04/26/12; Accepted: 06/02/12

<http://dx.doi.org/10.4161/cib.20980>

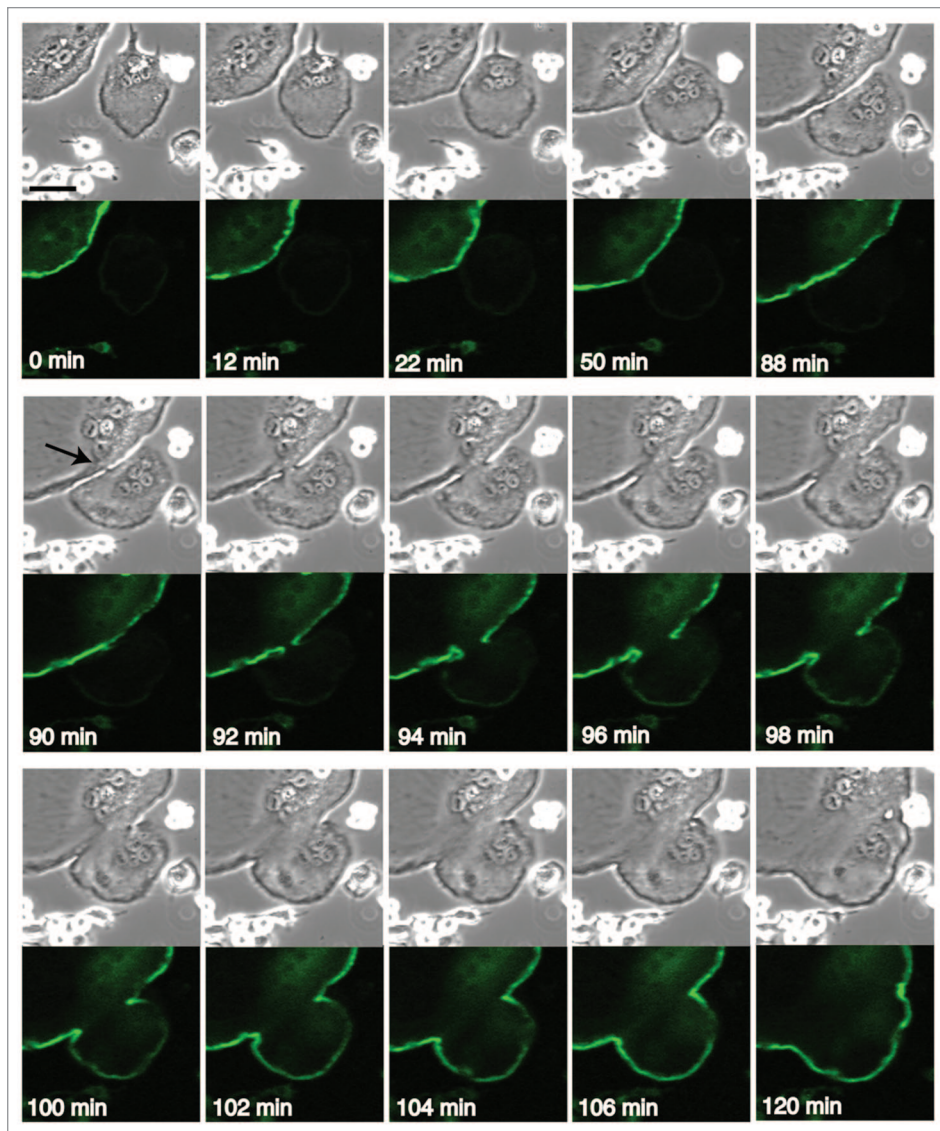


Figure 1. Cell fusion between EGFP-positive and EGFP-negative osteoclasts. RAW 264.7 cells were transfected with EGFP-actin and induced osteoclastogenesis by adding RANKL. The osteoclasts were processed for time lapse confocal microscopy as described.⁵ Images were retrieved every 2 min. Upper panel, DIC images. Lower panel, EGFP images. At 90 min, a stalk-like link appeared between two cells at the contact area (arrow). Bar, 50 μ m.

physical and chemical properties of the matrix on which the osteoclasts reside also change the dynamics of the podosome belt.¹⁵⁻¹⁷ Because the podosome itself exhibits the dynamic fission and fusion,¹⁸ the podosome belt probably inherits the dynamics from the podosome. In this study, we address the actin-based superstructures that appear at the contact site of two osteoclasts during the secondary fusion event.

The fusion of multinucleated osteoclasts can be monitored by following the dynamics of the podosome belt. RAW 264.7 cells were transfected with EGFP-actin, and osteoclastogenesis was induced by adding RANKL, as described previously.⁵ Thus, the transfected EGFP-actin labeled the podosomes and the podosome belt in the terminally differentiated osteoclast. **Figure 1** shows the fusion between EGFP-positive and EGFP-negative osteoclasts.

Time-lapse DIC imaging indicated that the two osteoclasts came into contact at time 12 min. The osteoclasts increased the degree of the cell contact from 22 min to 88 min, probably forming the zipper-like structure at the site of cell contact. At 90 min, a stalk-like link appeared between the two cells at the contact area, possibly representing a macroscopic stalk reminiscent of the microscopic stalk that is observed between the two apposed monolayers during the fusion of lipid bilayers.¹⁹ Interestingly, there was no discernible change in the podosome belt monitored by EGFP-fluorescence at 90 min. At 92 min, a gap occurred in the EGFP-fluorescence, indicating a local breakdown of the podosome belt. Thereafter, the gap widened in parallel with the distortion of the plasma membrane. At 96 min, a faint EGFP signal appeared in the EGFP-negative osteoclasts, becoming stronger and developing a clear belt at 102 min. This is probably due to the replacement of actin in the podosome belt of the EGFP-negative osteoclast with the incoming EGFP-labeled actin. With time, the fused osteoclast reshaped its podosome belt. Thus, as expected, the bulk mixing of the actin in the attached osteoclasts occurred after the fusion of the plasma membranes. The disappearance of the podosome belt at the fusion site is in agreement with the notion that the reorganization of the actin superstructure at the site of cell contact is intimately coupled with the fusion of the plasma membranes.

We next examined the fine structure of the cell surface of osteoclasts.

A DIC image showed that an osteoclast had numerous processes at the cell periphery (**Fig. 2A**). A DIC image of the zipper-like structure showed that the two cells were linked with numerous bridges at the cell contact site (**Fig. 2B**). These results raise the possibility that the recognition by the processes at the cell surface might trigger the formation of the zipper-like structure at the site of cell contact.

Transmission electron microscopy revealed that the plasma membranes in the zipper-like structure attached to each other via a discontinuous interface (**Fig. 2C**). In some cases, the apposed plasma membranes looked fuzzy, possibly suggesting the local merger of the plasma membranes (**Fig. 2D**). Thin bundles of actin filaments were observed in the merged region. Using scanning electron microscopy, Anderegge et al.²⁰ showed a clear image

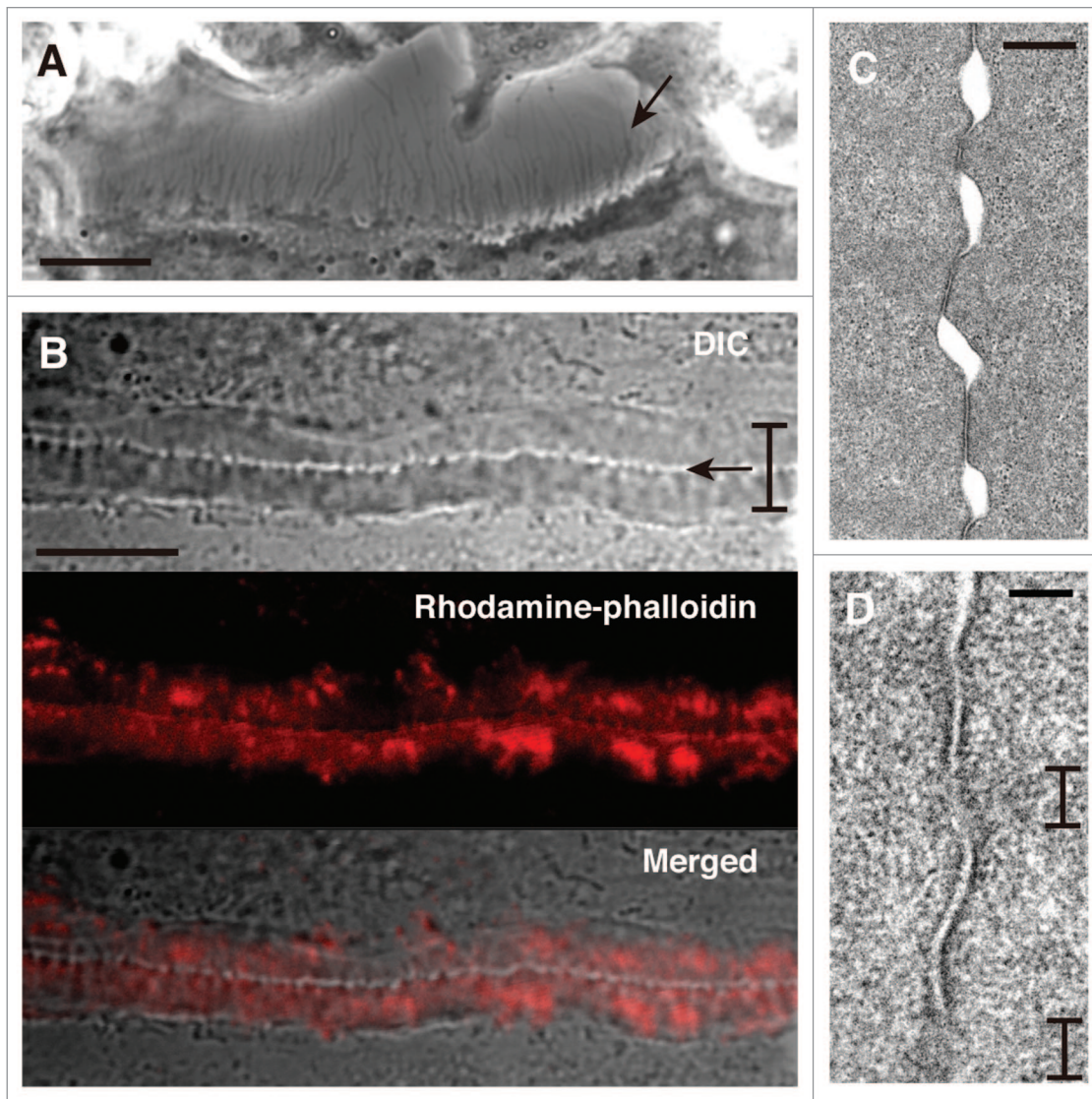


Figure 2. Fine structure at the site of cell contact between osteoclasts. (A) DIC image of osteoclast at day 4. The image shows the space between two osteoclasts. An osteoclast at lower position extends many thin processes at the cell surface (arrow). Bar, 10 μm . (B) The interface of two osteoclasts forms the zipper-like structure. Bracket indicates the short axis of the zipper-like structure. Arrow indicates the apparent physical links at the interface of two osteoclasts in the zipper-like structure. Upper, DIC image. Middle, rhodamine-phalloidin staining. Lower, merged image. Bar, 10 μm . (C) Transmission electron microscopy of the interface of two osteoclasts. Two osteoclasts attach to each other with gaps. Bar, 500 nm. (D) Apposed plasma membranes often contain fuzzy areas. Brackets indicate the fuzzy area. Bar, 100 nm.

of the actin bundles perpendicularly aligned across the long axis of the podosome belt and argued that the generation of the actin bundles in the podosome belt was due to the interplay between the podosome core domain and integrin-containing adhesion domain. Because the zipper-like structure also makes such domain arrangements,⁵ a similar mechanism could produce the actin bundles running across the cell contact site in the zipper-like structure.

We have to stress that the fusion mediated by the zipper-like structure is not a fixed mode of fusion between osteoclasts. Filopodium-mediated osteoclast fusion illustrates the sequence of cell-cell recognition, an intermediate stage, fusion of the cell bodies, and the reshaping of the fused cell (Fig. 3A). An osteoclast with a long filopodium was exploring a fusion partner at

time 0 min. At 2 min, the filopodium recognized a fusion partner and the filopodium then linked the two cells and became thicker and shorter. This intermediate stage exhibits a morphological similarity to so-called tunneling nanotubes, transient functional connections between cells separated by a long-distance.^{21,22} The cell bodies of the two osteoclasts began to fuse at 42 min, and the reshaping of the fused cell body had finished by 70 min. In this type of osteoclast fusion, the podosome belts in the two osteoclasts maintained their independence until the fusion of the cell bodies (Fig. 3B and from time 0 min to 40 min), and the fusion of the podosome belts occurred after the disappearance of the linked filopodium (Fig. 3B and time 40 to 44 min). Thus, osteoclasts use at least two machineries for cell-cell interaction during *in vitro* secondary fusion. Importantly, both types of

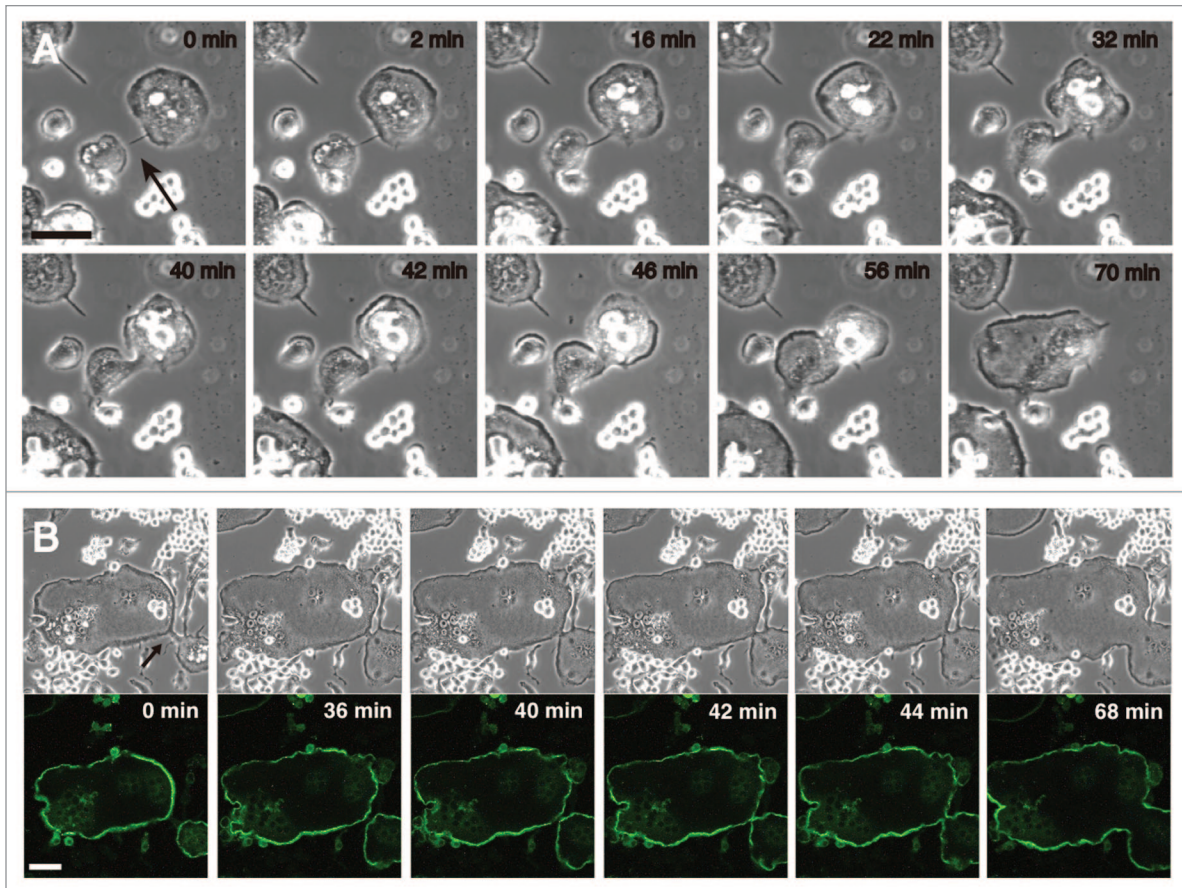


Figure 3. Filopodium-mediated fusion of osteoclasts. (A) DIC imaging of the filopodium-mediated fusion between osteoclasts. RAW 264.7 cells were induced osteoclastogenesis by RANKL. Time-lapse recordings delineate the sequence of cell-cell recognition, an intermediate stage, fusion of the cell bodies, and the reshaping of the fused cell. See text for details. The arrow indicates the filopodium. (B) Dynamics of podosome rings during the filopodium-mediated fusion. RAW 264.7 cells were transfected with EGFP-actin and induced osteoclastogenesis by RANKL. At time 0 min, two osteoclasts were linked with a filopodium (arrow). Two podosome belts in the linked cells maintained their independence until the fusion of the cell bodies. Images were retrieved every 2 min. Upper panel, DIC images. Lower panel, EGFP images. Bars, 50 μ m.

secondary fusions involve a lag between the cell-cell recognition and the membrane fusion (Figs. 1 and 3A). During this time, the two precursor osteoclasts probably exchange information via their actin-based superstructures. Further studies are necessary to resolve when and how osteoclasts use each actin superstructure during secondary fusion.

Although osteoclast fusion appears to be homotypic, Mensah et al.²³ presented evidence of the heterotypic nature of the fusion. Signals elicited by RANKL differentiate the single population of mononuclear precursors into two populations: DC-STAMP^{low} and DC-STAMP^{high} cells. Fusion between DC-STAMP^{low} and DC-STAMP^{high} produces larger cells than the fusion between DC-STAMP^{low} cells. In this regard, it is interesting to compare the expression level of surface DC-STAMP of the precursor cells with the appearance of the zipper-like structure during both primary and secondary cell fusions.

The reassembly of the podosomes to the new superstructures appears to create new functions. The ring-like arrangement of the podosome belt acquires the ability to seal the encircled area to generate the ruffled border membrane. The rearrangement of the podosome belt to the zipper-like structure might enable the

cells to create a physical path to exchange information during cell fusion. Thus, osteoclasts use podosomes as building blocks to cope with new tasks by rearranging their configuration in local areas.

Materials and Methods

Materials. The reagents used were obtained from the following sources: α -MEM, (WAKO, #135-15175); fetal bovine serum (FBS) (Sigma); rhodamine-phalloidin (Molecular Probes, #R415); and recombinant mouse sRANKL (PeproTech, #315-11).

Osteoclastogenesis. RAW 264.7 cells were seeded on a glass coverslip (Fisher Scientific, #12-545-82) placed in a 24-well culture dish at $1-2 \times 10^4$ cells in 0.5 ml α -MEM, 10% FBS, antibiotics, 0.1 mM non-essential amino acids, and 100 ng/ml sRANKL and cultured to induce osteoclastogenesis. Under these conditions, RAW 264.7 cells formed matured osteoclasts with the podosome belts by day 4. For confocal microscopy, the cells were fixed with 4% paraformaldehyde in PBS for 30 min, permeabilized with 0.5% NP-40 in PBS for 15 min, and blocked with 1% BSA in PBS for 1 h. The fixed cells were then incubated

with Rhodamine-phalloidin for 30 min. Confocal images were obtained using Olympus IX71 (Olympus).

Electronmicroscopy. RAW 264.7 cells were seeded on a 35 mm glass bottom dish with grids (Matsunami, #D111505) at 1.5×10^4 cells in 0.5 ml α -MEM, 10% FBS, antibiotics and 100 ng/ml RANKL and cultured for 3 d. The cells were fixed with 2% glutaraldehyde, 2% paraformaldehyde in 0.1 M PBS (pH 7.4) at 37°C for 15 min. The specimen was further fixed with 2% glutaraldehyde in 0.1 M PBS (pH 7.4) at 4°C. The cells were postfixed with OsO_4 , dehydrated and embedded in Quetol-812 (Nissin EM, #340). The glass was dissolved by incubating with hydrofluoric acid at room temperature for 20 min. Seventy nm thick sections were obtained by cutting parallel to the substratum. Sectioning was performed between 0.5 to 0.6 μm high from the substratum. The sections were stained with uranyl acetate and lead citrate. Photographs were taken on JEM-1200EX (JOEL) at 80 kV.

Live-cell imaging. Time-lapse confocal images were obtained with an Olympus FV10i (Olympus). RAW264.7 cells were

plated on a 35 mm glass bottomed culture dish (MatTek, #P35G-0-14-C). The cells were then transfected with EGFP-actin (Clontech, #632453) using the FuGENE HD transfection reagent (Roche) according to the protocol provided and allowed to differentiate into osteoclasts. The culture medium was supplemented with 100 ng/ml RANKL just before each recording. The retrieved images were processed with Photoshop CS (Adobe, CA).

Disclosure of Potential Conflicts of Interest

No potential conflicts of interest were disclosed.

Acknowledgements

We thank Y. Nonomura, T. Suda and N. Takahashi for their encouragement. The preliminary part of this work was performed at Keio University. This work was supported in part by Grants-in Aid for Challenging Exploratory Research [19659387] and The Fugaku Trust For Medicinal Research to J.T.

References

1. Suda T, Takahashi N, Udagawa N, Jimi E, Gillespie MT, Martin TJ. Modulation of osteoclast differentiation and function by the new members of the tumor necrosis factor receptor and ligand families. *Endocr Rev* 1999; 20:345-57; PMID:10368775; <http://dx.doi.org/10.1210/er.20.3.345>.
2. Vignery A. Macrophage fusion: the making of osteoclasts and giant cells. *J Exp Med* 2005; 202:337-40; PMID:16061722; <http://dx.doi.org/10.1084/jem.20051123>.
3. Kukita T, Wada N, Kukita A, Kakimoto T, Sandra F, Toh K, et al. RANKL-induced DC-STAMP is essential for osteoclastogenesis. *J Exp Med* 2004; 200:941-6; PMID:15452179; <http://dx.doi.org/10.1084/jem.20040518>.
4. Yagi M, Miyamoto T, Sawatani Y, Iwamoto K, Hosogane N, Fujita N, et al. DC-STAMP is essential for cell-cell fusion in osteoclasts and foreign body giant cells. *J Exp Med* 2005; 202:345-51; PMID:16061724; <http://dx.doi.org/10.1084/jem.20050645>.
5. Takito J, Nakamura M, Yoda M, Tohmonda T, Uchikawa S, Horiuchi K, et al. The transient appearance of zipper-like actin superstructures during the fusion of osteoclasts. *J Cell Sci* 2012; 125:662-72; PMID:22349694; <http://dx.doi.org/10.1242/jcs.090886>.
6. Yonemura S, Itoh M, Nagafuchi A, Tsukita S. Cell-to-cell adherens junction formation and actin filament organization: similarities and differences between non-polarized fibroblasts and polarized epithelial cells. *J Cell Sci* 1995; 108:127-42; PMID:7738090.
7. Cavey M, Lecuit T. Molecular bases of cell-cell junctions stability and dynamics. *Cold Spring Harb Perspect Biol* 2009; 1:2998; PMID:20066121; <http://dx.doi.org/10.1101/cshperspect.a002998>.
8. Vasioukhin V, Bauer C, Yin M, Fuchs E. Directed actin polymerization is the driving force for epithelial cell-cell adhesion. *Cell* 2000; 100:209-19; PMID:10660044; [http://dx.doi.org/10.1016/S0092-8674\(00\)81559-7](http://dx.doi.org/10.1016/S0092-8674(00)81559-7).
9. Linder S, Aepfelbacher M. Podosomes: adhesion hotspots of invasive cells. *Trends Cell Biol* 2003; 13:376-85; PMID:12837608; [http://dx.doi.org/10.1016/S0962-8924\(03\)00128-4](http://dx.doi.org/10.1016/S0962-8924(03)00128-4).
10. Jurdic P, Saltel F, Chabadel A, Destaing O. Podosome and sealing zone: specificity of the osteoclast model. *Eur J Cell Biol* 2006; 85:195-202; PMID:16546562; <http://dx.doi.org/10.1016/j.ejcb.2005.09.008>.
11. Zaidel-Bar R, Itzkovitz S, Ma'ayan A, Iyengar R, Geiger B. Functional atlas of the integrin adhesome. *Nat Cell Biol* 2007; 9:858-67; PMID:17671451; <http://dx.doi.org/10.1038/ncb0807-858>.
12. Schiller HB, Friedel CC, Boulegue C, Fässler R. Quantitative proteomics of the integrin adhesome show a myosin II-dependent recruitment of LIM domain proteins. *EMBO Rep* 2011; 12:259-66; PMID:21311561; <http://dx.doi.org/10.1038/embor.2011.5>.
13. Chabadel A, Bañon-Rodríguez I, Cluet D, Rudkin BB, Wehrle-Haller B, Genot E, et al. CD44 and beta3 integrin organize two functionally distinct actin-based domains in osteoclasts. *Mol Biol Cell* 2007; 18:4899-910; PMID:17898081; <http://dx.doi.org/10.1091/mbc.E07-04-0378>.
14. Destaing O, Saltel F, Géminard JC, Jurdic P, Bard F. Podosomes display actin turnover and dynamic self-organization in osteoclasts expressing actin-green fluorescent protein. *Mol Biol Cell* 2003; 14:407-16; PMID:12589043; <http://dx.doi.org/10.1091/mbc.E02-07-0389>.
15. Nakamura I, Takahashi N, Sasaki T, Jimi E, Kurokawa T, Suda T. Chemical and physical properties of the extracellular matrix are required for the actin ring formation in osteoclasts. *J Bone Miner Res* 1996; 11:1873-9; PMID:8970888; <http://dx.doi.org/10.1002/jbmr.5650111207>.
16. Saltel F, Destaing O, Bard F, Eichert D, Jurdic P. Apatite-mediated actin dynamics in resorbing osteoclasts. *Mol Biol Cell* 2004; 15:5231-41; PMID:15371537; <http://dx.doi.org/10.1091/mbc.E04-06-0522>.
17. Geblinger D, Addadi L, Geiger B. Nano-topography sensing by osteoclasts. *J Cell Sci* 2010; 123:1503-10; PMID:20375065; <http://dx.doi.org/10.1242/jcs.060954>.
18. Evans JG, Correia I, Krasavina O, Watson N, Matsudaira P. Macrophage podosomes assemble at the leading lamella by growth and fragmentation. *J Cell Biol* 2003; 161:697-705; PMID:12756237; <http://dx.doi.org/10.1083/jcb.200212037>.
19. Yang L, Huang HW. Observation of a membrane fusion intermediate structure. *Science* 2002; 297:1877-9; PMID:12228719; <http://dx.doi.org/10.1126/science.1074354>.
20. Anderegg F, Geblinger D, Horvath P, Charnley M, Textor M, Addadi L, et al. Substrate adhesion regulates sealing zone architecture and dynamics in cultured osteoclasts. *PLoS One* 2011; 6:28583; PMID:22162778; <http://dx.doi.org/10.1371/journal.pone.0028583>.
21. Rustom A, Saffrich R, Markovic I, Walther P, Gerdes HH. Nanotubular highways for intercellular organelle transport. *Science* 2004; 303:1007-10; PMID:14963329; <http://dx.doi.org/10.1126/science.1093133>.
22. Watkins SC, Salter RD. Functional connectivity between immune cells mediated by tunneling nanotubes. *Immunity* 2005; 23:309-18; PMID:16169503; <http://dx.doi.org/10.1016/j.immuni.2005.08.009>.
23. Mensah KA, Ritchlin CT, Schwarz EM. RANKL induces heterogeneous DC-STAMP(lo) and DC-STAMP(hi) osteoclast precursors of which the DC-STAMP(lo) precursors are the master fusogens. *J Cell Physiol* 2010; 223:76-83; PMID:20039274.